INSTITUTE OF PHYSICS PUBLISHING SUPERCONDUCTOR SCIENCE AND TECHNOLOGY

Supercond. Sci. Technol. **18** (2005) 1391–1395 doi:10.1088/0953-2048/18/10/025

Magnetic flux penetration in MgB_2 thin films produced by pulsed laser deposition

M Roussel[1], A V Pan[1], A V Bobyl[2], Y Zhao[1], S X Dou[1] and T H Johansen[2]

[1] Institute for Superconducting and Electronic Materials, University of Wollongong, Northfields Avenue, Wollongong, NSW 2522, Australia
[2] Department of Physics, University of Oslo, PO Box 1048, Blindern, 0316 Oslo, Norway

E-mail: roussel@uow.edu.au

Received 1 July 2005, in final form 10 August 2005
Published 5 September 2005
Online at stacks.iop.org/SUST/18/1391

Abstract
Two types of MgB_2 thin films produced by pulsed laser deposition with different *in situ* and *ex situ* sintering routes have been studied. Using the magneto-optical (MO) imaging technique, the magnetic flux penetration behaviour in the films has been investigated. In the case of the *in situ* film, the MO observations reveal conventional flux jumps below the corresponding threshold temperature, whereas in the case of the *ex situ* film the flux jumps appear to take the form of unusual, structurally driven 'blob'-like patterns. The underlying structural features of the films have been investigated by scanning electron and atomic force microscopy. The critical current density dependence on applied magnetic field obtained from magnetization measurements is consistent with the local behaviour of the magnetic flux, as well as with flux pinning properties expected from the obtained crystalline structure of the *ex situ* film and the amorphous-like surface of the *in situ* film. On the basis of these structural and electromagnetic observations, a mechanism for the structurally driven, spatially reproducible flux jumps is proposed.

(Some figures in this article are in colour only in the electronic version)

1. Introduction

The discovery of superconductivity in the binary compound MgB_2 [1] has led to numerous studies in order to understand and improve the superconducting properties of this material. The high activity in this research field is governed by various beneficial properties exhibited by this material [2]. These features include high critical temperature $T_c \simeq 39$ K, a simple structure, a relatively large coherence length, and high critical current densities J_c, in zero and high applied magnetic fields, H_a, as well as a relatively low price compared to high T_c superconductors. All these aspects make MgB_2 a very attractive superconductor for possible applications.

However, at low temperatures and low fields MgB_2 superconductors exhibit a significant depression of their J_c (by up to 50%) due to magnetic flux jumps. This instability, which is most pronounced in thin films where the flux jumps take the form of dendritic structures [3–6], limits the practical applications of this material. Consequently, it is of vital importance to understand these abrupt events of flux motion, their origin and possible differences in the behaviour of MgB_2 films prepared by various methods.

In this work we have studied flux jumps in high quality MgB_2 films prepared by two different processes. In the next section we describe the preparation conditions of what we call *in situ* and *ex situ* MgB_2 thin films produced by pulsed laser deposition (PLD). Also the various experimental techniques used for the study will be outlined. In section 3 we compare electromagnetic and structural properties of the *in situ* and *ex situ* films. In section 4 we focus on the magnetic flux penetration in the *ex situ* film, where we found a quite different behaviour compared to the common dendritic patterns seen in MgB_2 films. Finally, we summarize the results obtained in this work.

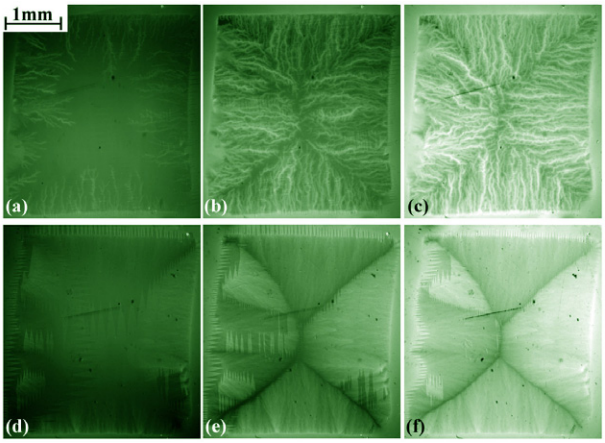

Figure 1. Magnetic flux penetration in the *in situ* film: (a) $T = 4$ K, $H_a = 3.4$ mT, (b) $T = 4$ K, $H_a = 8.5$ mT, (c) $T = 4$ K, $H_a = 25.5$ mT, (d) $T = 15$ K, $H_a = 3.4$ mT, (e) $T = 15$ K, $H_a = 10.2$ mT, (f) $T = 15$ K, $H_a = 27.2$ mT. In this figure and the following, saw-tooth-like lines correspond to magnetic domain walls of the indicator film. These domain walls are irrelevant to the work presented in this paper; hence, they will not be considered hereafter.

Table 1. Film preparation and characteristics.

	In situ	*Ex situ*
Sintering process	Sintered in the PLD chamber: 685 °C for 1 min	Sintered in a furnace: 900 °C for 30 min
T_c in zero field	28 K	36 K
Film topology	≈300 nm thick with 500 nm height droplet, very rough	≈300 nm thick, smoother

2. Experimental details

The MgB_2 films were fabricated on Al_2O_3 substrates by the PLD technique with the target aligned with the substrate. For the samples referred to as *in situ* films, we first deposited a film using a stoichiometric MgB_2 target under a low pressure of argon gas and maintaining the substrate at 250 °C. This was followed by the deposition of a magnesium cap layer about 800 nm thick. The sample was then annealed in the deposition chamber at 685 °C in argon for 1 min under 1 atm pressure. The films referred to as *ex situ* were prepared by depositing a boron precursor film in vacuum. Then, the boron film was wrapped in tantalum foil and sealed in a stainless steel tube together with magnesium pellets. The tube was subsequently heat-treated for 30 min at 900 °C in a furnace. More details of the synthesis of both kinds of films is described elsewhere [7, 8]. For this work, one typical sample of each kind was studied. Their preparation details and important characteristics are summarized in table 1.

The magneto-optical (MO) imaging technique was used to study the local magnetic flux behaviour. This technique is based on the Faraday effect occurring in a thin single-crystalline layer of bismuth substituted yttrium iron garnet grown by liquid phase epitaxy on gadolinium gallium garnet substrate under conditions that give an in-plane magnetization in the MO active layer. This so-called indicator film was placed directly on top of the superconducting sample. In a polarizing

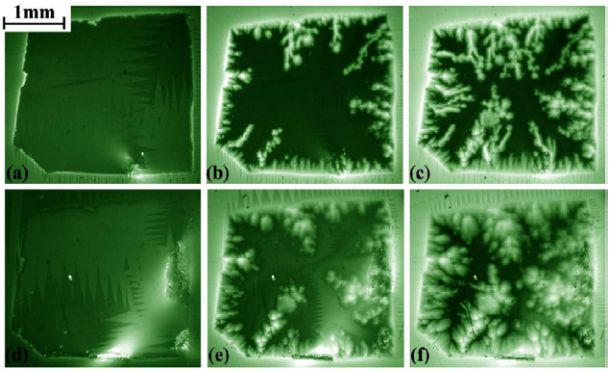

Figure 2. Magnetic flux penetration in the *ex situ* film: (a) $T = 4$ K, $H_a = 3.4$ mT, (b) $T = 4$ K, $H_a = 17$ mT, (c) $T = 4$ K, $H_a = 25.5$ mT, (d) $T = 15$ K, $H_a = 3.4$ mT, (e) $T = 15$ K, $H_a = 17$ mT, (f) $T = 15$ K, $H_a = 27.2$ mT. The bright region in the lower right corner is due to stress in the indicator film and do not correspond to a high magnetic flux density area.

microscope (reflection mode) with crossed polarizer and analyzer, an image is formed where the variation in brightness represents the distribution of the perpendicular flux density component. An extensive and recent review on MO imaging can be found in [9]. In all our MO imaging experiments, the external magnetic field was applied perpendicular to the MgB_2 film using a resistive coil. The MO images were recorded while keeping a constant temperature after the samples had been cooled below T_c in zero field.

Magnetization measurements were performed on the same samples in order to compare and connect the local and global behaviour of the magnetic flux. The magnetization hysteresis loops were measured using a SQUID magnetometer. From the width of these loops, ΔM, we obtained a J_c of the films from the critical state formula, [10]:

$$J_c = \frac{\Delta M(H)}{a \times (1 - \frac{a}{3b})}$$

where the surface area of the film is $2a \times 2b$ (m^2) with $a \leqslant b$ being the width and the length of the films, respectively.

The surface topography and the thickness of the films were obtained by atomic force microscopy (AFM) and scanning electron microscopy (SEM). The film thickness was $d = 300$ nm for both samples.

3. Comparison of *ex situ* and *in situ* films

3.1. Magneto-optical observations

Figures 1 and 2 show MO images of the *in situ* and *ex situ* films, respectively. The pictures are taken at constant temperatures while the applied magnetic field is slowly increased. At 4 K the penetration behaviour is governed by abrupt macroscopic motion of vortices creating dendrite-like structures in both films. However, the dendrites clearly appear to be different in each film.

(i) In the *in situ* film, the dendrites are numerous and they developed more branches and have thinner and longer cores than in the other film.

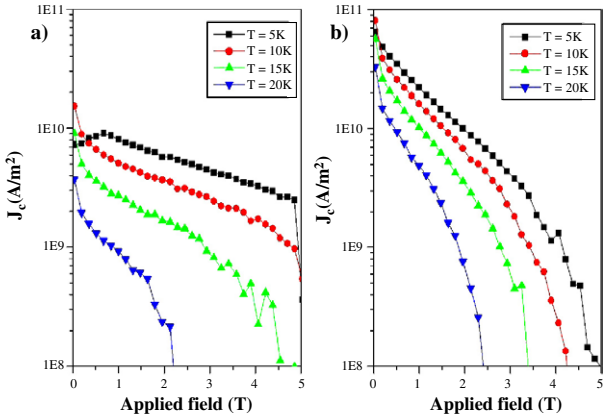

Figure 3. J_c dependence on the applied magnetic field (a) in the *in situ* film and (b) in the *ex situ* film.

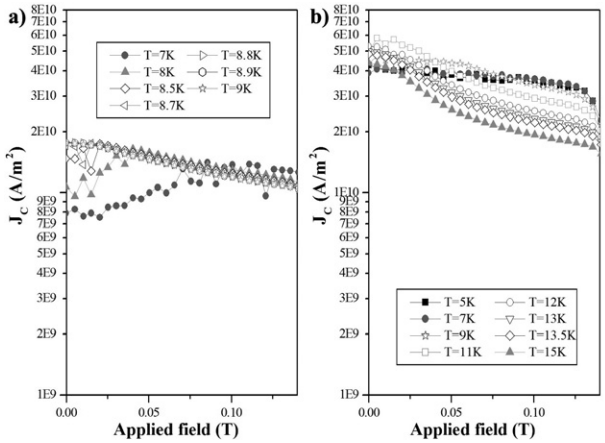

Figure 4. The same J_c field dependence as shown in figure 3 for low fields up to 0.14 T only (a) in the *in situ* film and (b) in the *ex situ* film.

(ii) The *ex situ* film exhibits fewer, and considerably thicker, 'blob'-like structures.

Above a threshold temperature of $T_t \sim 8$ K, the magnetic flux penetration becomes gradual in time for both films. However, spatial features of the penetration remain different. In the *ex situ* film, the flux front is still not smooth, whereas in the *in situ* film the overall penetration pattern is regular as predicted by the critical-state model.

The abrupt dendritic penetration seen in the *in situ* film below the threshold temperature is commonly observed in superconducting films, and was reported earlier for MgB_2 [4, 5, 11] or Nb [12]. Such structures were also observed in films of $YBa_2Cu_3O_x$, but only when the instability is triggered by a laser pulse [13]. The origin of such abrupt events is presumably the heat dissipation associated with the motion of the Abrikosov vortices, a local heating of the superconductor which in turn leads to further depinning and motion of vortices toward the sample centre where the local magnetic flux density is lower. At low temperatures, where the heat capacity is sufficiently small, this results in a thermal run-away with dramatic consequences [3, 11]. Moreover, there is also a threshold magnetic field H_d which has to be exceeded before the first flux dendrites appear [14]. This is also fully consistent with the well known thermo-magnetic flux jump behaviour in bulk superconductors.

From numerous studies done on dendritic avalanches [3–6, 11, 15], several general characteristics emerge: they have an ultra-fast formation; appear at random places; their shape cannot be reproduced from one experiment to another, which indicates their structural independence from sample defects; once formed, they stay frozen and do not change with increasing field and disappear above a certain temperature threshold, usually around 10 K for MgB_2. The structures observed in our *ex situ* film do not conform to all these characteristics as will be discussed in section 4.

3.2. Global magnetization measurements

Figure 3 shows how J_c of the two films depends on applied fields up to 5 T. Details of the behaviour at fields below 0.14 T are seen in figure 4. A depression of J_c is observed at $T \leqslant 9.0$ K for the *in situ* film and at $T \leqslant 13$ K for the *ex situ* film. These reductions in apparent J_c can be understood as the result of the dendritic flux jumps seen with MO imaging.

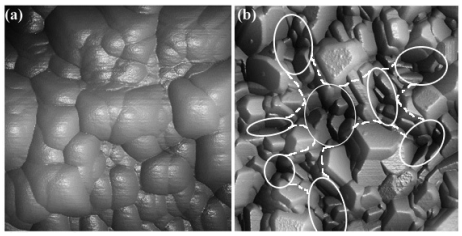

Figure 5. AFM pictures of (a) the *in situ* and (b) the *ex situ* films; the areas covered are $0.5 \times 0.5\ \mu m^2$ and $2 \times 2\ \mu m^2$ respectively; the white circles in (b) correspond to incomplete holes on the surface of the film and the dashed lines to shallow valleys.

Note, however, that the threshold temperatures found in the magnetization measurements are higher than in the MO experiments. There are several possible reasons for this. First, the sample mounting in the two experiments is different. In particular, the presence of a metallic layer on the MO indicator film is known to suppress the formation of dendrites. Second, the J_c obtained from global magnetometry is derived from both the ascending and descending field branches. Since dendrites are formed more easily during field decrease, most likely due to the additional heat released during flux antiflux annihilation, we find here a higher threshold temperature.

At zero field, the *ex situ* film exhibits a much higher $J_c(0\,T)$ of 9×10^{10} A m^{-2} at $T = 10$ K as compared to the *in situ* film where $J_c(0\ T, 10\ K) \simeq 1.5 \times 10^{10}$ A m^{-2}. However, in increasing magnetic fields the J_c drops much faster in the *ex situ* film than in the *in situ* sample. This $J_c(H_a)$ behaviour indicates that the *in situ* film has many more defects suitable for strong pinning than the *ex situ* sample.

3.3. Structural characterization of the films

To get more insight into the different behaviour of $J_c(H_a)$ in the two types of film, their surface morphology was studied using AFM and SEM. As seen in figure 5 the *ex situ* film has a

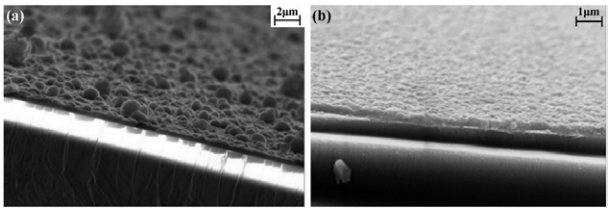

Figure 6. SEM pictures of (a) the *in situ* and (b) the *ex situ* films.

better crystallized structure with large hexagonal-like grains, as compared to the *in situ* film possessing a rather smooth but granular structure. We find no favoured crystallographic orientation in any of these surfaces. Note the scale difference in the two AFM images. More details about the microstructure of both films and its effect on their superconducting properties can be found in [16].

A careful study of the AFM data shows that the landscape of the *ex situ* sample exhibits an array of regions with reduced film thickness randomly scattered over the entire film surface. Encircled in figure 5(b) are a number of such 'incomplete holes'. The diameter of these features varies from 0.2 to 0.8 μm. Their depth is of the order of 100 nm, which amounts to one-third of the total thickness of the superconducting layer. Some of the incomplete holes are as deep as 150 nm.

The SEM pictures in figure 6 show the surface topography of each sample at larger scales. Here the *ex situ* surface is noticeably more homogeneous than in the *in situ* film, where numerous droplets are found over its entire surface area.

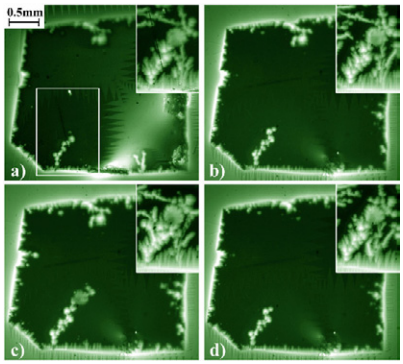

Figure 7. MO images of the same *ex situ* film during four different sets of measurements. The applied fields are (a) 10.2 mT, (b) 8.5 mT, (c) 10.2 mT, and (d) 11.9 mT. All the pictures were taken at $T = 4$ K. The insets show the area corresponding to the area marked by the white rectangle in figure (a) for the same set of measurements respectively but at higher fields ($H_a = 34$ mT).

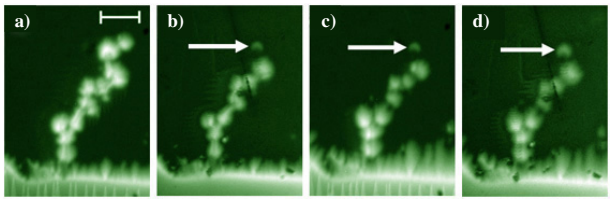

Figure 8. MO images of the same *ex situ* film during four different sets of measurements; the applied field is about 10.2 mT and the temperature is 4 K for images (a) and (b), 8 K for image (c) and 15 K for image (d); the scale bar corresponds to 0.2 mm. The arrow marks a 'run-away' flux spot.

4. Discussion

Whereas the formation of the dendritic structures seen in our *in situ* film possesses essentially all the characteristics reported in previous papers on the subject, our *ex situ* film displays elements of a distinctly new behaviour. Shown in figure 7 are examples of unexpected features of the dendrites observed in the *ex situ* film. The four images were taken during four separate experiments with the same sample, all done at $T = 4$ K, and after ramping the applied field to $H_a = 10.2$, 8.5, 10.2 and 11.9 mT. The insets in each panel show MO images from the same four experiments but at the higher field of 34 mT. It is evident that the observed structures reproduce the same flux pattern from one experiment to another, contradicting the expectation for dendritic flux jumps as described previously [4, 5]. Another new feature, seen from the insets, is that the irregular flux patterns clearly continue to evolve as the applied field increases. Furthermore, a comparison of the flux penetration behaviour below and above the threshold temperature, see figure 8, shows that the flux patterns tend to reproduce the same structures. This behaviour suggests that the fast forming finger structures decorated with 'blob'-like patterns is strongly governed by defects present in the sample. We believe these features result from the distribution of incomplete holes shown in figure 5(b).

Several groups have studied the influence of hole arrays on the flux penetration in superconducting films. In the works [17] and [18] the holes had a diameter of the same order of magnitude as the holes in our *ex situ* film, and vortices were shown to strongly interact with such defects. We expect this to be the case also for incomplete holes [18], as in our *ex situ* film. It has been shown that holes act like collectors of magnetic flux when their diameter is larger than the superconductor's coherence length. However, MO imaging studies of films patterned with different hole lattices pointed out that the periodicity of the observed flux patterns can be much larger than the periodicity of the hole lattice [17, 19]. This is indeed similar to our results, as the typical distance between the observed 'flux blobs' is much larger than the distance between the incomplete holes in the *ex situ* film. However, the penetration described in [17] was shown to be independent of the structural features of the sample, and also spatially non-reproducible, as a result of a perfect film and hole lattice. In contrast, our *ex situ* sample shows flux patterns which are spatially reproducible both below and above the threshold temperature, suggesting that a new mechanism plays a crucial role in this film.

In addition to the incomplete holes randomly distributed over the entire film surface, we also found that they are interconnected by shallower valleys (figure 5). Thus, the sample consists basically of a network of vortex collecting defects, connected by channels, which act as lines of easy flux penetration. Therefore, this network creates a dominant guided flux motion even during course of the flux jumps, and hence removes the commonly observed irreproducibility of the phenomenon.

Consequently, the observed 'blob'-like penetration patterns are likely to follow this process: the external flux is focused at edge defects, and as the external field is increased flux-jump avalanches occur. However, instead of forming dendrites of random shapes and at random locations, the flux is 'guided' through the incomplete holes interconnected by numerous shallow valleys. The flux penetration patterns are expected to be similar below and above the flux-jump threshold with the only difference that above the threshold the process is gradual, whereas below the threshold this process is abrupt, exhibiting flux jumps as observed in our experiments.

A reproducible 'run-away' flux spot marked by the arrows in figure 8 could imply that the flux pinning is quite small in the *ex situ* film. Thus, after a field increase, the flux is collected in incomplete holes where the pinning level for vortices or multi-quantum flux bundles can be significantly higher, whereas the high purity crystalline structure easily expels the flux into 'blob'-like holes due to the local recovery of the Meissner state after a flux-jump avalanche passage event. This description is consistent with the $J_c(H_a)$ dependence measured for the *ex situ* film. A high zero-field critical current density and its rapid degradation as a function of the field are characteristic to relatively high purity samples with the flux pinning (e.g., by flux collecting holes) effective at low fields only.

It is also interesting to note that the 'common' dendritic avalanches as described at the beginning of this section and in [3–6, 11, 15] are virtually non-existent in the *ex situ* film. This quasi-absence is most probably caused by the fact that the observed abrupt 'blob' penetration events prevent the local magnetic flux from reaching the threshold value H_d in most areas of the sample.

5. Conclusion

The *ex situ* and *in situ* MgB_2 thin films were prepared by the PLD technique under different conditions. A significant difference in the local magnetic behaviour of the flux penetration in the films has been explained with the help of the combination of global and local structural, as well as electromagnetic, experiments. The MO images show that the magnetic flux penetration in both films below the corresponding thresholds is governed by abrupt thermo-magnetic flux-jump avalanches corresponding to the anomalous noise observed in the J_c-field curves. The penetration in the *in situ* film is consistent with the dendrite penetration widely discussed in the literature. In contrast, the flux penetration into the *ex situ* film has been found to occur by unusual structurally driven flux jumps. These 'blob'-like features strongly interact with the underlying incomplete hole structure of this film. These interactions lead to spatially reproducible flux avalanches.

References

[1] Nagamatsu J, Nakagawa N, Muranaka T, Zenitani Y and Akimitsu J 2001 *Nature* **410** 63–4
[2] Buzea C and Yamashita T 2001 *Supercond. Sci. Technol.* **14** R115–46
[3] Altshuler E and Johansen T H 2004 *Rev. Mod. Phys.* **76** 471–87
[4] Johansen T H, Baziljevich M, Shantsev D V, Goa P E, Galperin Y M, Kang W N, Kim H J, Choi E M, Kim M S and Lee S I 2001 *Supercond. Sci. Technol.* **14** 726–8
[5] Johansen T H, Baziljevich M, Shantsev D V, Goa P E, Galperin Y M, Kang W N, Kim H J, Choi E M, Kim M S and Lee S I 2002 *Europhys. Lett.* **59** 599–605
[6] Bazijevich M, Bobyl A V, Shantsev D V, Altshuler E, Johansen T H and Lee S I 2002 *Physica* C **369** 93–6
[7] Zhao Y, Ionescu M, Pan A V and Dou S X 2003 *Supercond. Sci. Technol.* **16** 1–6
[8] Zhao Y, Ionescu M, Horvat J and Dou S X 2004 *Supercond. Sci. Technol.* **17** S482–5
[9] Jooss Ch, Albrecht J, Kuhn H, Leonhardt S and Kronmüller H 2002 *Rep. Prog. Phys.* **65** 651–788
[10] Chen D X and Goldfarb R B 1989 *J. Appl. Phys.* **66** 2489–500
[11] Shantsev D V, Goa P E, Barkov F L, Johansen T H, Kang W N and Lee S I 2003 *Supercond. Sci. Technol.* **16** 566–70
[12] Durán C A, Gammel P L, Miller R E and Bishop D J 1995 *Phys. Rev.* B **52** 75–8
[13] Leiderer P, Boneberg J, Brüll P, Bujok V and Herminghaus S 1993 *Phys. Rev. Lett.* **71** 2646–9
[14] Barkov F L, Shantsev D V, Johansen T H, Goa P E, Kang W N, Choi E M and Lee S I 2003 *Phys. Rev.* B **67** 064513
[15] Bobyl A V, Shantsev D V, Johansen T H, Kang W N, Kim H J, Choi E M and Lee S I 2003 *Appl. Phys. Lett.* **80** 4588–90
[16] Zhao Y, Ionescu M, Roussel M, Pan A V, Horvat J and Dou S X 2005 *IEEE Trans. Appl. Supercond.* **15** 3261–4
[17] Vlasko-Vlasov V, Welp U, Metlushko V and Crabtree G W 2000 *Physica* C **341–348** 1281–2
[18] Raedts S, Silhanek A V, Van Bael M J, Jonckheere R and Moshchalkov V V 2004 *Physica* C **404** 298–301
[19] Kolesnik S, Vlasko-Vlasov V, Welp U, Crabtree G W, Piotrowski T, Wróbel J, Klimov A, Przyshupski P, Skoskiewicz T and Dabrowski B 2000 *Physica* C **341–348** 1093–4